caMelot

UNDERSTANDING CHARGE, MASS AND HEAT TRANSFER IN FUEL CELLS FOR TRANSPORT APPLICATIONS

Grant agreement no.: 875155

Start date: 01.01.2020 – *Duration*: 36 months
Project Coordinator: Dr. Thor Aarhaug - SINTEF

DELIVERABLE REPORT

M2.1 – WATER TRANSPORT IN THIN IONOMERIC MATERIALS AND MEMBRANES	
Due Date	April 30, 2022
Author (s)	David Harvey and Jiri Hrdlicka
Workpackage	2
Workpackage Leader	David Harvey (M14 onwards), Jiri Hrdlicka (M1 up to M14)
Lead Beneficiary	FAST Simualtions (M14 onwards), TUC (M1 up to M14)
Date released by WP leader	June 30, 2022
Date released by Coordinator	June 30, 2022

DISSEMINATION LEVEL		
PU	*Public*	*X*
PP	*Restricted to other programme participants (including the Commission Services)*	
RE	*Restricted to a group specified by the consortium (including the Commission Services)*	
CO	*Confidential, only for members of the consortium (including the Commission Services)*	

NATURE OF THE DELIVERABLE		
R	*Report*	*X*
P	*Prototype*	
D	*Demonstrator*	
O	*Other*	

SUMMARY	
Keywords	*Ionomer model, water transport, PEMFC, Performance, Water Uptake*
Abstract	*An improved ionomeric material and membrane sub-model is developed for implementation in a broader unit cell performance model. The sub-model implements the water transport mechanisms based on the chemical potential gradient, liquid water pressure gradient, and electro-osmotic drag. Further, the model implements a sorption methodology to capture the water content vs activity relationship for thin membrane materials and demonstrates the capability of the approach to predict ex-situ testing methods such as Dynamic Vapour Sorption (DVS).*
Public abstract for confidential deliverables	

REVISIONS			
Version	**Date**	**Changed by**	**Comments**
1	30 June 2022	David Harvey	Draft Release
2	6 December 2022	David Harvey	Added Executive Summary

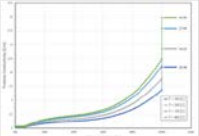# WATER TRANSPORT IN THIN IONOMERIC MATERIALS AND MEMBRANES

CONTENT

1 EXECUTIVE SUMMARY

An improved physical model of a membrane has been developed which implements additional physics to predict the water content vs. relative humidity relationship for a perflourinated sulphonic acid membrane. The model uses dynamic vapour sorption measurements to establish the adsorption and desorption from the membrane and the equilibrium water contents. The model has been used to simulate the dynamic vapour sorption measurement and has demonstrated the ability to capture the transient behaviour of the system (criteria #1 for verification and validation); further the equilibrium water contents using the adsorption/desorption methodology is comparable to the equilibrium water content vs. relative humidity relationships that are extracted from the dynamic vapour sorption data (criteria #2 for verification and validation). The original model for the water uptake from water vapour which was implemented in the model was based on the water content vs relative humidity relationship measured by (Springer, Zawodsinski, & Gottesfield., 1991); the original model's implementation simply used the reported relationship for equilibrium water content vs. relative humidity as a inputted value and therefore had no predictive capability for the adsorption, desorption, and transport processes which will change in relative importance as the thickness and composition of the membrane is altered. A schematic of the physical differences between the original model and improved physical model are shown in Table 1 below.

Table 1: Added Capabilities in Improved vs. Original Model

2 INTRODUCTION

The development of membrane models and their progressive refinement has been the topic of many years of on-going research and development. Starting in 1991, Springer et al developed one of the foundational works that has continued to be cited to this day with respect to the relationship between the vapour activity of water and the water uptake of PFSA-based polymeric membranes. Bernardi and Verbrugge (1992) published their development on a hydraulic model describing the movement and transport of water within the ionomeric membranes, Janssen & Overvelde published their "Net Drag Coefficeint" model in 2001 with Janssen contributing a supplementary publication in the same year on the use of Concentrated Solution within a Phenomenological Model, in 2004 Weber and Newman published a pair of papers that set-out a mixed potential, irreversible thermodynamics model and introduced a chemical potential based approach for describing water movement within the MEA, and Monroe in 2009 introduced a Vaporization-Exchange Model to describe the sorption processes occurring in the ionomeric materials. Through all of this work there have been numerous observations and insight gained in the mechanisms, various ways to represent the physics, and the failings of various approaches.

As PEMFC technology has continued to advance and the ionomeric materials used in today's state-of-the-art fuel cell MEAs are now sufficiently thinner and more highly optimized than the materials used circa 2015 and earlier; it has become equality important to ensure that the theoretical understanding, modelling approaches, and available analysis methods remain consistent with these significantly improved material sets. To that end, this development work as part of the CAMELOT project has set-out to improve the existing descriptions contained within FAST-FC, which were based on the descriptions set out in 2015 and earlier, such that FAST-

FC is capable to describing the performance and operational behaviours for the newest, state-of-the-art ionomeric materials.

3   SCOPE

The scope of this work is on the development of a sub-model which describes water transport mechanisms within the ionomeric materials within a proton exchange membrane fuel cell, specifically the model will focus on the prediction of the water content, the sorption processes, and the effect of the water on the proton movement mechanisms.

4   DISCUSSION

The development of the improved membrane and ionomer sub-model was undertaken to improve upon the existing model included within FAST-FC as published in (Harvey, 2017). This pre-existing model described water within the membrane to be in a "dissolved" state and that the movement of the dissolved water was driven via gradients in concentration. The uptake and loss of water from the membrane and ionomer was described through a set of source terms that distinguished the phase of water in the bulk pores (i.e. water in liquid or vapour phase) and applied rates of absorption and desorption which were determined based on literature data which was available at that time. The pre-existing model was focused on the state-of-the-art materials at that time and did not include any sophistication in the way the absorption and desorption rates were described; although (Shah, Kim, Sui, & Harvey, 2007) did perform a sensitivity study within a transient framework which indicated the relative sensitivity of the model results to these parameters.

In laying out the improved approach proposed within the CAMELOT project, it is useful to first consider the phenomenological observations of water movement within the Membrane Electrode Assembly and, subsequently, the structure of the MEA and how that relates to the water movement. During fuel cell operation, the internal conditions within an MEA can result in a situation where local water exists in a vapour only, mixed vapour-liquid, or liquid only state. The latter liquid-only state would be rare and likely exist only in extremely flooded situations whereas the vapour only and mixed vapour-liquid states would be the general case and highly likely under normal operation. Given that the vapour-only and the mixed states of water are anticipated to be general case normal operation, it remains that it is necessary to consider the effect of both the vapour and liquid states on the uptake and transport within the ionomeric materials of the MEA; a schematic of the various modes of water transport within the ionomeric materials of the catalysts and membrane is shown in Figure 1.
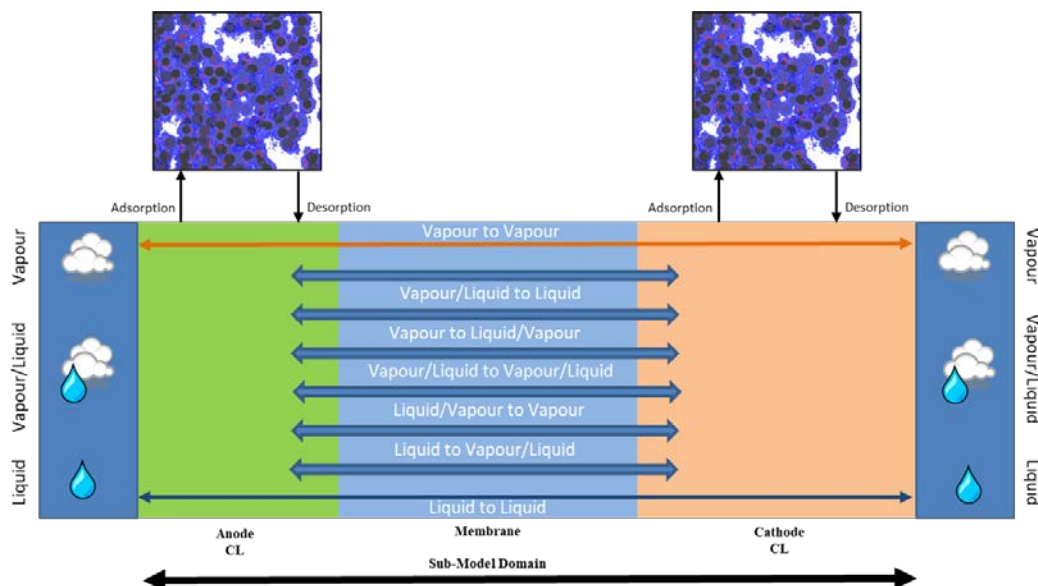

Figure 1: Schematic of the modes of water transport within the catalyst layers and transport within the ionomeric phase

Phenomenologically, water transport has been observed to occur where there is a (1) partial pressure difference between the anode and cathode compartments, (2) liquid pressure difference between the anode and cathode compartments, and (3) temperature difference between the anode and cathode compartments. However, these general observations are convoluted by the process of sorption and desorption of water from the bulk state in the pores of the catalyst layers into and out of the dissolved state within the ionomeric materials. These processes, combined with structural interactions of water with the polymer itself, complicate the observations between ultra-thin membranes and the previous state of the art materials in that the movement of water across the MEA may be dominated by either the sorption/desorption or dissolved water transport within the ionomeric materials; this balance could also further shift either way due to the interaction with the operating conditions within the flow field of the unit cell.

To address the challenges and improve on the previous implementation within FAST-FC, the improved membrane and ionomer sub-model was developed first as a stand-alone model and then subsequently implemented within a test-bed version of FAST-FC based on a one-dimensional implementation of the broader framework. The development and implementation of the stand-alone ionomeric sub-model was used to apply and evaluate the results of the equation system with ex-situ analysis methods, such as Dynamic Vapour Sorption, for the purpose of verifying and validating the sub-model's capability to capture ex-situ behaviours in water uptake and transport; while, the implementation of the sub-model within the FAST-FC test bed was used determine its effect within the fully coupled equation system which is used to simulate in-situ environment and predict the performance of MEAs.

4.1 Water Transport Sub-Model

The improved ionomeric water transport sub-model considers water to be driven by two primary mechanisms: (1) Pressure driven flux and (2) Chemical Potential driven flux. These two modes are consistent with the work of (Weber & Newman, 2004) and those transport modes are then further combined with modelling approaches which include consideration for the sorption behaviour of water by ionomeric materials; specifically, that behaviour is applied to improve the description for sorption within the catalyst layers.

4.1.1 Liquid Pressure Driven Water Transport

In the previous discussions, it was stated that phenomenological observations indicate that water can be transported across ionomer materials due to an established gradient in liquid water pressure between the anode and cathode compartments. That flux of water across the ionomeric materials then arises to a liquid pressure gradient and has been described in the sub-model using the following governing equation:

$$\epsilon_{\text{ion}} \frac{f_w}{RT} \frac{\partial p_l}{\partial t} + \nabla \cdot \left(-\alpha_\ell V_w \nabla p_\ell \right) = S_i$$

In this equation, p_ℓ represents the liquid pressure and has units of pressure in bar, ϵ_{ion} represents the volume fraction of ionomer within component of interest (in the case of the membrane, this would be 1 or the fraction represented by the ionomer relative to the structural reinforcement), R is the universal gas constant, and T is the local temperature.

The variable fw represents the volume fraction of "dissolved" water within the ionomeric materials and is determined using the following form:

$$f_w = \frac{\lambda V_w}{V_m + \lambda V_w}$$

Where fw is unitless, λ is the water uptake, Vm is the equivalent molar mass of the ionomer, and Vw is the molar volume of liquid water.

α_ℓ represents the effective diffusivity of water in the ionomer in a liquid-equilibrated state, has units of [mol^2/(J m s)] and is given by,

$$\alpha_\ell = \frac{k_{\text{sat}}}{\tilde{\mu}_w V_w^2}\left(\frac{f_w}{f_\ell}\right)^2$$

Where f_ℓ is the volume fraction of water, f_w, evaluated at $\lambda_\ell = 22$, k_{sat} is the absolute hydraulic permeability of the ionomeric material which has a value of 1.8 x 10^{-18} [m^2], and μ_w is the dynamic viscosity of liquid water.

The chemical potential of water was determined using the Sutherland law and is valid from 2°C up to 95°C,

$$\tilde{\mu}_w = 10^{-3}\,\text{Pa s} \exp\left(-3.63148 + \frac{542.05\,\text{K}}{T - 144.15\,\text{K}}\right)$$

Within the ionomeric membrane, the source term, S$_i$, is zero as there is no source of liquid pressure within the ionomeric membrane itself. However, in the catalyst layers the generation of liquid pressure relates to the evaporation and condensation process and the source term, S$_i$, can be described as S$_i$ = S$_{ec}$, where S$_{ec}$ is, in general, an evaporation and condensation process which is described as a departure from equilibrium saturation. With sub-model implemented as part of the broader framework, S$_{ec}$ uses the equation included within the liquid water transport formulation within the bulk transport of liquid water within the porous media (hence no further explanation of S$_{ec}$ is included here and is instead referenced to the current test-bed implementation of FAST-FC).

The inclusion the evaporation and condensation rate as the source term for the pressure driven flux remains an on-going area of improvement and work in order to determine if inclusion is mechanistically correct; based on observations this may not be the case and it may be more mechanistically correct that the pressure driven flux only relates to the local liquid pressure which exerts a normal force on the surface of the ionomeric membrane and that the catalyst ionomer does not functionally contribute to this mode due to its dendrite-like structures covering and mingling with the carbon support, catalyst nanoparticles, and additives that may be introduced with the intent to control the liquid water movement. This is supported based on, e.g., (Karan, 2019) and (A Kusoglu, 2017), where the sorption of water into the ionomer within the catalyst layers is much lower ($\lambda_{\text{max,CL}} \approx 5$ compared to $\lambda_{max,m} \approx 14$) compared to the ionomer that comprises the membrane. Such a decrease could be attributed to the dendrite-like ionomer structure within the catalyst layers, which unlike the ionomer in membrane, does not form the moieties (inverted micelles) but remains mostly untangled. In this arrangement the phase separation and subsequent formation of a hydrophilic domain containing a network of channels does not occur for the ionomer within the catalyst layers as described by the effect of the liquid pressure on the fraction of expanded channels which is described in the next section such that the transport of ions and water is mediated by a different set of values and reduced transport mechanisms as compared to the ionomeric membrane.

4.1.2 Chemical Potential Driven Water Transport

From Figure 1, phenomenological observations were also indicative of water movement due to differences in the partial pressure of water vapour. The flux of water across the ionomeric materials due to observed differences in partial pressure and temperature are described within the sub-model using a chemical potential driven flux of water with a governing transport equation which can be written as:

$$\epsilon_{\text{ion}}\frac{c_w}{RT}\frac{\partial u}{\partial t} + \nabla \cdot \left(\epsilon_{ion}\left[-\frac{\kappa\xi_v}{F}\nabla\varphi + (1-s)\left(-\alpha_v - \frac{\kappa\xi_v^2}{F^2}\right)\nabla\mu_w + s\left(-\alpha_\ell - \frac{\kappa\xi_\ell^2}{F^2}\right)V_w\nabla p_\ell\right]\right) = S_i$$

Where, μ_w represents the chemical potential of has units of [J/mol], ϵ_{ion} represents the volume fraction of ionomer within the component of interest (in the case of the membrane, this would have a value of 1 or the fraction represented by the ionomer relative to the structural reinforcement as mentioned previously), φ represents the protonic potential, and F is Faraday's constant.

κ, ξ and α are the protonic conductivity, electroosmotic drag coefficient and effective diffusivity, respectively, and the subscript ℓ refers to values for liquid equilibrated ionomer materials and the subscript v refers to the same but for the vapor equilibrated case.

c_{w} represents the molar concentration of water and can be determined using the equivalent molar mass of the ionomer, V_{m}, and the molar volume of liquid water, V_{w}, which are described previously:

$$c_{\mathrm{w}} = \frac{\lambda}{V_{\mathrm{m}} + \lambda V_{\mathrm{w}}}$$

The variable s refers to a blending variable which was introduced by (Weber & Newman, 2004) in attempt to reconcile the mixed mode cases which are described in Figure 1. This blending variable is described to represent the ratio of expanded channels within the ionomer and is determined as a function of the critical radius, r_{c}, and mean radius, r_{avg}, of the ionomeric material's internal pores:

$$s = \frac{1}{2}\left[1 - \mathrm{erf}\left(\frac{\ln(r_{\mathrm{c}}) - \ln(r_{\mathrm{avg}})}{0.3\sqrt{2}}\right)\right]$$

The critical pore radius of the ionomeric materials is related to the surface tension of the water, γ, the contact angle, θ, and the local pressure of liquid water, p_{ℓ}, such that it can be calculated using the following form:

$$r_{\mathrm{c}} = -\frac{2\gamma\cos(\theta)}{p_{\ell}}$$

Effectively, this methodology results in a shifting of the driving force between the chemical potential gradient driven flux and that driven by the liquid pressure gradient.

The protonic conductivity of the ionomeric materials, κ, is determined using:

$$\kappa = 50\,\frac{\mathrm{S}}{\mathrm{m}}\,(f_{\mathrm{w}} - 0.06)^{1.5}\exp\left[-\frac{-15\ \mathrm{kJ/mol}}{R}\left(\frac{1}{303.15\ \mathrm{K}} - \frac{1}{T}\right)\right]$$

This form is as reported by (Weber & Newman, 2004) and uses f_{w} rather than λ as the predictor for the relationship between water content and the mobility/conductivity of the protons. Practical comparisons between the relationship originally measured by Springer and this form yield that this form predicts a value of $\lambda = 22$ at a fraction of water within the membrane, f_{w}, of approximately 0.42. Other works, such as (Vetter & Schumacher, 2019), have explored this correlation and adapted it to their datasets; in particular, (Vetter & Schumacher, 2019) implemented a value of 116 S/m based on a reference measurement temperature of 353.15 K as opposed to 50 S/m with a reference measurement temperature of 303.15K which is shown above.

The electro-osmotic drag coefficient, ξ, is distinguished based on the whether the reference for the ionomeric materials is to a vapour equilibrated or liquid equilibrated state; recalling that the blending parameter, s, allows for a contribution simultaneously from mixed state conditions. The definition for the electro-osmotic drag coefficient in the vapour equilibrated state, ξ_{v}, is determined to be practically equal to one due to the low values of f_{w} for the vapour only equilibrated state. This is not the case for the liquid equilibrated state where the value of ξ_{ℓ} is determined according to the following:

$$\xi_{\ell} = 2.55\exp\left[-\frac{-4\ \mathrm{kJ/mol}}{R}\left(\frac{1}{303.15\ \mathrm{K}} - \frac{1}{T}\right)\right]$$

This form is a typical Arrhenius corrected form and presumes a change in the electro-osmotic drag with temperature based on a value of 2.55 at a reference temperature of 303.15 K.

The value of the effective diffusivity related to the liquid equilibrated state of the ionomeric materials, α_ℓ, is as reported in the previous section related to the flux driven by the gradient in liquid water pressure, p_ℓ, whereas the value for the effective diffusivity related to the vapour equilibrated state of the ionomeric materials is determined using a form which relates it to the diffusivity of water that is consistent with a chemical potential driving force (as opposed to concentration):

$$\alpha_v = \frac{c_w}{RT} \frac{D_\mu}{(1 - x_w)}$$

Where, the molar concentration of water, c_w, has the definition as given previously and the molar fraction of water, x_w, was determined from a relationship to the water content of the ionomeric material, λ:

$$x_w = \frac{\lambda}{1 + \lambda}$$

The diffusivity of water in the ionomeric materials relative to a chemical potential driving force and corrected using an Arrhenius form takes on the following form:

$$D_\mu = 1.8 \times 10^{-9} \frac{m^2}{s} f_w \exp\left[-\frac{-20 \text{ kJ/mol}}{R}\left(\frac{1}{303.15 \text{ K}} - \frac{1}{T}\right)\right]$$

This form, as reported by (Weber & Newman, 2004), highlights three key dependencies; the first dependency is to the water content, f_w, which explains the observation that water movement decreases with decreasing water content due to stronger interactions between the "dissolved" water and the sulfonic acid sites, the second dependency relates to the value for the activation energy which implies that the diffusion coefficient in the ionomer materials is lower than that in bulk water due to the interactions with the ionomeric structure/sulfonic acid sites, and third dependency is the effect of temperature which adds the outcome that as the temperature changes so should the mobility of the "dissolved" water molecules due to changes in energy levels and the ability to overcome the energy barrier related to movement within the ionomeric structure.

The source term, S_i, is zero within the membrane as there is not uptake of water within the volume of the ionomeric membrane itself. Within the catalyst layers, the source term represents the uptake of water due to sorption and evaporation/condensation (the inclusion of the latter remains an on-going area of improvement and work in order to determine if inclusion is mechanistically correct) such that it can be described in the anode and cathode catalyst layers, respectively, as:

$$S_{ACL} = S_{ad} + S_{ec}$$

$$S_{CCL} = S_{ad} + S_{ec} + S_R$$

Implicitly, the form of S_{CCL} indicates that the production of water from the electrochemical reaction occur within the ionomeric phase surrounding the catalytic reaction sites. This is an interpretation that is included based on the strict assumption that catalyst reaction sites are inactive unless a triple phase boundary is achieved. In reality, this may be too idealistic in that it has been postulated by others that the triple phase boundary can be achieved in part by ionomer but also in part through a thin water layer where protons may travel or migrate thus activating a greater degree of catalytic surface area. For simplicity in this model, the adherence to an ionomeric activated triple phase boundary will be used and relaxation of this description will be address as part of the future work.

With respect to the form of the source terms, S_R is the electrochemical production of water on the cathode and is described as part of the broader model framework and as such is not described here as there is not deviation from the already reported form. The form of S_{ec} is similar to the discussion in the previous section in that the source of water due to evaporation and condensation

is part of the broader framework which has previously been reported and is therefore not described again in the sub-model. The discussion related to the accuracy of mechanistic description and the inclusion of S$_{ec}$ remains accurate also for its inclusion here as well. The value of the source term related to the sorption process, S_{ad}, is an improvement over the previous sub-model within FAST-FC and it relates the observed elements of the isotherms for uptake that can be observed and compared with Dynamic Vapour Sorption and other ex-situ tests. The description for S_{ad} is as follows, based on an implementation of an equilibrium switch to drive the sorption as a departure from equilibrium based on the local conditions within the catalyst layers:

$$S_{ad} = a_{ion}h_{vd}(\mu_{wv} - \mu_{wd}) + a_{ion}h_{ld}(\mu_{wl} - \mu_{wd})$$

Where, a_{ion} represents the volumetric density of ionomer interfacial area in m^2/m^3, h_{vd} and h_{ld} are mass transfer coefficients related to sorption from the vapour and liquid phases, respectively; μ_{wv} and μ_{wl} are the chemical potential of the vapour water and liquid water respectively in the pore space and μ_{wd} is the chemical potential of the dissolved water in the ionomeric material.

The source term S_{ad} is configured such that it is positive when absorption occurs and negative when desorption occurs; this is in part also controlled by the forms of h_{vd} and h_{ld} which are written, adapting the work of (Shah, Kim, Sui, & Harvey, 2007), as follows:

$$h_{\mathrm{vd}} = 0.5k_{\mathrm{d}}(1-S)\left(1 + \frac{\mathrm{mol}}{\mathrm{J}}\mathrm{sign}(\mu_{\mathrm{wd}} - \mu_{\mathrm{w}})\right) + 0.5k_{\mathrm{a}}(1-S)\left(1 - \frac{\mathrm{mol}}{\mathrm{J}}\mathrm{sign}(\mu_{\mathrm{wd}} - \mu_{\mathrm{w}})\right)$$

Where k_{d} represents the desorption rate, k_{a} the adsorption rate, μ_{wd} the chemical potential of the dissolved water, and μ_{w} the chemical potential of water outside the ionomer.

S represents the liquid saturation within the interstitial pore space in the catalyst layers and can be written as:

$$S = \frac{V_\ell}{V_{\mathrm{pore}}}$$

In the presence of liquid water in the pores (S>0), the mass transfer coefficient related sorption from the liquid phase, h_{ld}, can be written as:

$$h_{\mathrm{d}\ell} = \frac{1}{4}k_a\left(1 + \frac{S - S_*}{|S - S_*|}\right)\left(1 - \frac{\mathrm{mol}}{\mathrm{J}}\mathrm{sign}(\mu_{\mathrm{wd}} - \mu_{\mathrm{w}})\right) + \frac{1}{2}k_{\mathrm{d}}\left(1 - \frac{\mathrm{mol}}{\mathrm{J}}\mathrm{sign}(\mu_{\mathrm{wd}} - \mu_{\mathrm{w}})\right)$$

The sorption rates are given by:

$$k_{\mathrm{d}} = 1.6 \times 10^{-5}\frac{\mathrm{mol}^2 \mathrm{s}}{\mathrm{kg\ m}^4}f_{\mathrm{w}}\exp\left[-\frac{-20\ \mathrm{kJ/mol}}{R}\left(\frac{1}{303.15\ \mathrm{K}} - \frac{1}{T}\right)\right]$$

$$k_{\mathrm{a}} = 4 \times 10^{-6}\frac{\mathrm{mol}^2 \mathrm{s}}{\mathrm{kg\ m}^4}f_{\mathrm{w}}\exp\left[-\frac{-20\ \mathrm{kJ/mol}}{R}\left(\frac{1}{303.15\ \mathrm{K}} - \frac{1}{T}\right)\right]$$

Where the activation energy of -20 kJ/mol is adopted from the temperature scaling of viscosity (2416 K = E_{act}/R). The scaling with water content has been taken from the definition of the mass transfer coefficients and replaced by the scaling with the volume fraction of water in the ionomer, f_w.

4.1.3   Implementation of a Revised Sorption Approach

Although a solid choice near 30 °C, the Springer's sorption isotherm (Springer, Zawodsinski, & Gottesfield., 1991) does not cover other temperatures. In the presented model, the sorption isotherm from Takata et al. (Takata, Mizuno, Nishikawa, Fukada, & Yoshitake, 2007) has been selected because it approximates well the CAMELOT material set while involving temperature dependence and adjustable parameters obtainable by measurement and a mechanistic description rather than fitting. Compared to the approach of Weber &

Newman in (Weber & Newman, 2004), Takata's relation for the hydration number is an explicit relation, rather than a set of two nonlinear algebraic equations requiring an iterative solution.

Takata's sorption curve is described by:

$$\lambda = \frac{EW}{\rho_m M_w} Q + \lambda_0 + s(\lambda_\ell - \lambda_{\max})$$

and,

$$Q = \frac{A_L B_L p_w}{1 + A_L p_w}[1 + (n-1)(A_C p_w)^{n-1}]$$

Where, λ_0 is residual water that is present in membranes exposed in their history to water that can only be removed upon thermal decomposition of the membrane because it is solvating the sulfonic groups (Shimoaka, Wakai, Sakabe, Yamazaki, & Hasegawa, 2015). The parameter $\lambda_{\max}$ refers to $\lambda(1, T)$ and λ_ℓ is liquid-equilibrated water uptake (so far $\lambda_\ell = 22$ has been used, but value obtained from measurements should be used instead).

The parameters in Takata's sorption model have the following values

$$EW = 0.933 \text{ kg/mol @ 15 } \mu m \text{ and EW=1.017 kg/mol @ 10 } \mu m$$

$$A_L = 1.53 \times 10^{-10} \frac{1}{\text{Pa}} \exp\left[-\frac{-39 \text{ kJ/mol}}{RT}\right]$$

$$A_C = 2.40 \times 10^{-12} \frac{1}{\text{Pa}} \exp\left[-\frac{-46 \text{ kJ/mol}}{RT}\right]$$

$$B_L = 160 \frac{\text{kg}}{\text{m}^3 \text{ dry membrane}}$$

$$n = 5.15$$

$$p_w = \frac{RH}{100} p_w^{\text{sat}}, \qquad p_w^{\text{sat}} = 1 \text{ Pa} \exp\left(23.1963 - \frac{3816.44 \text{ K}}{T - 46.13 \text{ K}}\right)$$

When processing measurements (DVS and water uptake), it is convenient to express the lambda in terms of the volume fraction of water:

$$f_w = \frac{\lambda V_w}{V_m + \lambda V_w} \quad \rightarrow \quad \lambda = \frac{V_m}{V_w}\frac{f_w}{1 - f_w}$$

Similarly, water uptake, also referred to as the relative fraction of water can be defined in terms of f_w or λ:

$$W_w = \frac{m_w}{m_m} = \frac{f_w V \rho_w}{(1 - f_w)V \rho_m} = \frac{\rho_w}{\rho_m}\frac{f_w}{1 - f_w} = \frac{M_w}{M_m}\lambda$$

Again $M_m = EW$ and it is important to note that the last relation also clearly defines the units of λ.

Finally, the boundary values of the chemical potential need to be established. The partial molar Gibbs energy of water, which carries the meaning of the chemical potential of water can be expressed using the fundamental equation of chemical thermodynamics (Atkins & Paula, 2010, 9th edition):

$$d\mu_w = -S_w dT + V_w dp$$

where the partial molar entropy, $S_w = c_p/T$, can be integrated from selected reference conditions, T_{ref} and p_{ref}, to the operating conditions of interest, T_o and p_o, yielding the following:

$$\mu_w(T_o, p_o) - \mu_w(T_{\text{ref}}, p_{\text{ref}}) = -\int_{T_{\text{ref}}}^{T_o} \frac{c_p(T)}{T} dT + \int_{p_{\text{ref}}}^{p_o} \frac{M_w}{\rho_w} dp$$

Where c_p is the molar heat capacity and $\rho_{w\ell}$ is the density of liquid water.

Examining the definition set out by (Weber & Newman, 2004) for the chemical potential:

$$\mu = \mu_{ref} + RT\ln(a) + V_w p_\ell$$

It can seen that the first integral term on the corresponding to the temperature dependence of the chemical potential disappeared, i.e. was absorbed in the reference term. The pressure dependence term is split between the gas contribution, $V_{wg} = RT/p$, and liquid contribution, $V_{w\ell} = M_w/\rho_{w\ell}$, because the molar volume of water depends on the state of aggregation (phase).

As written, using the convention that the reference pressure for water vapor is the saturated water vapor pressure, an integral from the reference pressure to the saturated water vapor pressure is not explicitly accounted for and can be assumed to be also a part of the μ_{ref}. By the same token, the last term only deals with liquid pressure and must be tracked by integrating from reference pressure to the liquid pressure, through the use of the capillary pressure, with the integral from reference to saturated water vapor pressure being absorbed into the reference term.

As such, it can be concluded that:

$$\mu_w(T_o, p_o) = \mu_{w,ref} + RT_o\ln(a) + V_w(p_\ell - p_o)$$

with the liquid pressure defined as $p_\ell = p_0 - p_c$, where p_c is the capillary pressure given by a function such as the Leverett J-function; in the absence of liquid water, $p_c = 0$, $p_\ell = p_o$ and the liquid water contribution disappears.

The reference potential, μ_w, can be expressed as:

$$\mu_{w,ref} = \mu_w(T_{ref}, p_{ref}) - \int_{T_{ref}}^{T_o} \frac{c_p(T)}{T} dT + RT\ln\left(\frac{p_w^{sat}(T_o)}{p_{ref}}\right) + RT\ln\left(\frac{p_o}{p_w}\right) + V_w(p_o - p_{ref})$$

Because p_w corresponds to p_o under the given conditions, $RT\ln(p_o/p_w)$ could be zero.

The final aspect that must be defined is the value of the chemical potential under the reference conditions; unfortunately, trying to employ the equation of state for water from (Wagner & Pruß, 2002), which makes a common reference for solid, liquid and vapor water at the triple point cannot be reconciled with literature.

An alternative option is the formation molar Gibbs energy of water at some arbitrary reference temperature (cell operating temperature), e.g. $\mu_\ell^{ref} = -237.18$ kJ/mol or $\mu_v^{ref} = -228.59$ kJ/mol which are obtained at $T^{std} = 298.15$ K and $p^{std} = 101325$ Pa (Adachi, et al., 2010). Such values can be obtained using the NIST Webbook for water, oxygen and hydrogen:

For vapor,

$$\Delta_f H_v^{\emptyset} = -241.826 \pm 0.040 \frac{kJ}{mol}, \quad S_v^{\emptyset} = 188.835 \pm 0.010 \frac{J}{mol\,K}$$

and for liquid at 1 bar and 25 °C,

$$\Delta_f H_\ell^{\emptyset} = -285.830 \pm 0.040 \frac{kJ}{mol}, \quad S_\ell^{\emptyset} = 69.95 \pm 0.03 \frac{J}{mol\,K}$$

The Shomate equation can also be applied, with the coefficients tabulated in various sources:

$$c_p^{\emptyset} = A + Bt + Ct^2 + Dt^3 + E/t^2$$

where $t = T/1000$ K.

Using the Hess law:

$$\Delta_r H = -1H_{H_2} - 0.5H_{O_2} + 1H_{H_2O}$$

$$\Delta_r S = -1S_{H_2} - 0.5S_{O_2} + 1S_{H_2O}$$

$$\Delta_r G = \Delta_r H - T\Delta_r S$$

The molar Gibbs free energy in these forms corresponds to the reference chemical potential.

The reference values can be re-evaluated for other conditions using total differentials and constant values of molar entropy and molar volume of water as coefficients multiplying the temperature and pressure difference with respect to the reference conditions (Job & Herrmann, 2006):

$$\mu_{w\alpha} = \mu_{ref,\alpha} - s_{m,\alpha}(T - T_{ref}), \;\; \text{and} \;\; \mu_{w\alpha} = \mu_{ref,\alpha} + V_{m,\alpha}(p - p_{ref})$$

where subscript α refers to the state of aggregation and the corresponding reference value of the chemical potential, s_m is the molar entropy and V_m the molar volume.

The values of the molar entropy and molar volume can be evaluated at T_{ref} and p_{ref}, or elsewhere and, alternatively, a cubic fit may be used to provide a more precise value if necessary. Such procedure, albeit less accurate, is much more practical and easier to implement than the integration (the Shomate equation allows the use of explicit formulae).

The accuracy can be gauged by the comparison to the rigorous formula presented above. It should be noted that in a single-phase model (vapor-equilibration only), the choice of the reference chemical potential is completely arbitrary and $\mu_w^{ref} = 0$ J/mol has been used for the sake of simplicity, still yielding the proper range of activity (activity a has been locally calculated from the chemical potential to obtain local water uptake λ).

4.2   Charge Transport

As a result of the new water transport and sorption sub-model for the ionomeric materials and the strong interaction between the dissolved water content and the transport/mobility of the protonic charge carriers within the ionomeric materials, the transport equation governing the movement of the charge carriers within the ionomeric materials has also been updated.

4.2.1   Protonic Transport

Based on the modified form of the water transport sub-model for liquid pressure driven and chemical potential driven flux, the governing equation for proton transport within the ionomeric materials now takes the following form:

$$\nabla \cdot \left(-\kappa \nabla \varphi + \frac{\kappa}{F}[-\xi_\ell V_w \nabla p_\ell - (1-s)\xi_v \nabla \mu_w] \right) = S_{i,rxn}$$

In this form there now exist three driving forces, the first term describes the movement of protons due to a potential difference, the second term reflects the effect of the movement of dissolved water due to a liquid pressure gradient on the movement of protons, and the third term describes the effect of the movement of dissolved water due to a chemical potential gradient on the movement of protons.

All terms in the above equation have been defined previously in the other sections, with the exception of source term related to the generation or consumption of protons due to the electrochemical reactions, $S_{i,rxn}$, which occur on the anode and cathode. Within the membrane the value of $S_{i,rxn}$ is zero as in the performance model there are no reactions that are assumed to occur in the bulk of the membrane that could consume or generate protons. Within the two catalyst layers, the anode and cathode, the HOR and ORR reactions are occurring and used to define $S_{ACL,HOR}$ and $S_{CCL,ORR}$. These source terms are defined with the broader, previously reported framework of FAST-FC and will not be repeated here brevity.

5   EX-SITU VERIFICATION AND VALIDATION

The analysis of the output of the model implementation was done in two steps, the first step was the verification/comparison of the model theory together with characterisation experiments generated within the project and from literature sources; for the ionomeric sub-model described within this work, the verification

and comparison were initially done using sorption curves which correlated the gas phase activity of water vs the dissolved water held within the ionomeric phase, λ.

From Figure 2, we can observe that the data for 10 and 15µm thick membranes falls along the sorption model of Takata which has been implemented within this work. This highlights that the relationship between the local conditions and the total amount of uptake at steady state for the thinner membrane materials is well captured by the implemented sorption model adopted from Takata. For comparison, the original membrane sub-model took this relationship as an input rather than predicting it based on a sorption isotherm. Further, if a comparison is made between Figure 2 and Figure 3, it can clearly be observed that the Activity vs. Water Content relationship which was implemented in the original sub-model of FAST-FC would have been incapable of properly capturing the water content for the thinner membrane materials.
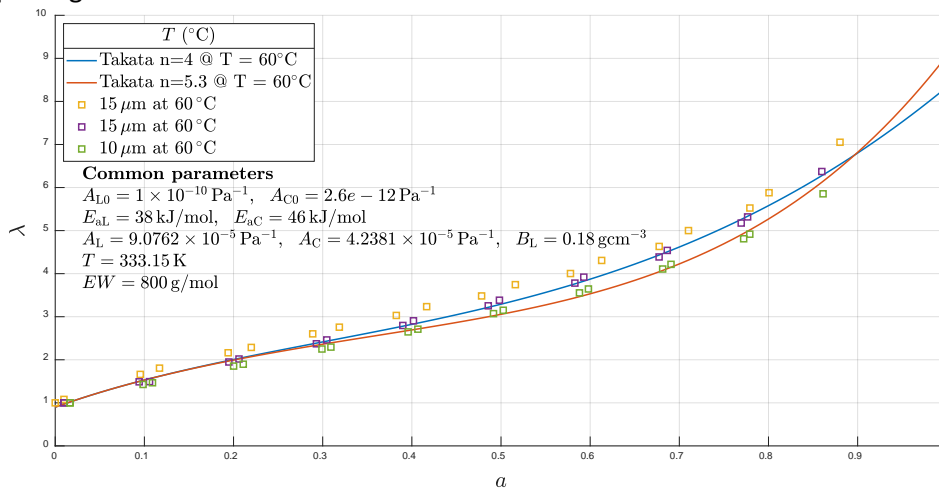

Figure 2: Activity vs. Water Content relationship predicted using the new sub-model based on the implementation of the sorption approach from Takata using n=4 or n=5.3 and compared to experimental results generated within the CAMELOT project.
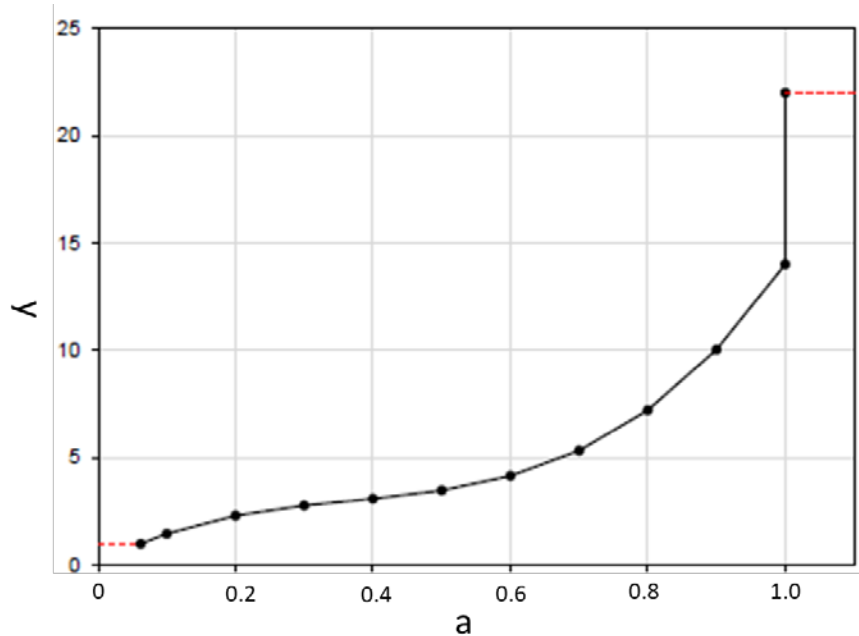

Figure 3: Activity vs. Water Content relationship input from original FAST-FC ionomeric sub-model3

From a validation perspective, the goal was to compare the ability of the model to capture the sorption behaviour using an ex-situ Dynamic Vapour Sorption measurement. Within the original ionomeric description implemented in FAST-FC, the sorption behaviour was unable to capture the behaviour. The primary reason for this was that the original equation set used the values from Figure 3 to assert the equilibrium water content and these equilibrium values do not match the accumulated water content in the plateau regions shown in

Figure 4. However, the improved ionomeric water transport and sorption model developed within the CAMELOT project has demonstrated the capability to capture both the shape of the behaviour (curvature observed in the relative mass fraction percentage of water in the ionomer during in the step-wise increase of relative humidity and step-wise decrease of the relative humidity in the DVS experiment); additionally, the model is also demonstrating the capability to capture the achievement of the steady-state plateau that occurs as the membrane sample goes the initial sorption and then the process slows down as the water content within the membrane stabilizes towards the equilibrium condition.
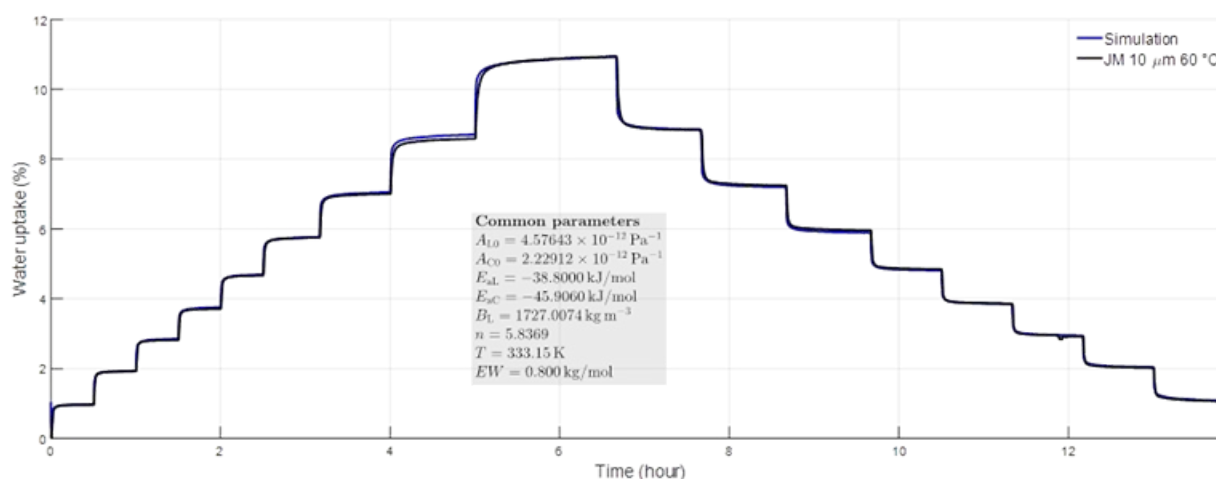

Figure 4: Comparison of Dynamic Vapour Sorption Measurements vs. the Predicted behaviour using the improved ionomeric water transport and sorption sub-model

6 CONCLUSIONS AND FUTURE WORK

A revised sub-model for water transport within ionomeric materials has been developed for FAST-FC which is based on a chemical potential and liquid pressure driven flux and includes a description for the sorption processes occurring within the catalyst layers. Initial verification of the sub-model with dynamic vapour sorption has shown promising capability to describe the water uptake process with additional validation upcoming on the predicted conductivities vs water content based on in-situ cell performance.

Future work on the sub-model will focus on the pressure-driven water flux and the mechanistic description/consistency of its implementation and connection to the chemical potential gradient driven flux and the effect of both modes on the movement of protons within both the ionomeric materials of the catalyst layers and membrane. On-going assessment and verification will be done in order to further ensure the mechanistic consistency and build up a broader validation data set on both an ex-situ and in-situ basis.

7 REFERENCES

A Kusoglu, A. W. (2017). New insights into perfluorinated sulfonic-acid ionomers. *Chemical Reviews*, 117(3):987–1104.

Adachi, M., Navessin, T., Xie, Z., Li, F., Tanaka, S., & Holdcroft, S. (2010). Thickness dependence of water permeation through proton exchange membranes. *Journal of Membrane Science*, 364(1):183–193.

Atkins, P., & Paula, J. d. (2010, 9th edition). *Physical Chemistry.* Oxford University Press.

Harvey, D. B. (2017). *Development of a Stochastically-driven, Forward Predictive Performance Model for PEMFCs.* Kingston: Doctoral Thesis, Queens University.

Job, G., & Herrmann, F. (2006). Chemical potential – a quantity in search or recognition. *Eur. J. Phys.* , 27, 353–371.

Karan, K. (2019). Interesting Facets of Surface, Interfacial, and Bulk Characteristics of Perfluorinated Ionomer Films. *Langmuir*, 35, 42, 13489–13520.

Shah, A., Kim, G., Sui, P., & Harvey, D. (2007). Transient non-isothermal model of a polymer electrolyte fuel cell. *Journal of Power Sources*, 163(2) Pages 793-806.

Shimoaka, T., Wakai, C., Sakabe, T., Yamazaki, S., & Hasegawa, T. (2015). Hydration structure of strongly bound water on the sulfonic acid group in a Nafion membrane studied by infrared spectroscopy and quantum chemical calculation . *Physical Chemistry Chemical Physics*, 17, 8843-8849.

Springer, T., Zawodsinski, T., & Gottesfield., S. (1991). Polymer electrolyte fuel cell model. *Journal of the Electrochemical Society*, 138(8):2334 – 2342.

Takata, H., Mizuno, N., Nishikawa, M., Fukada, S., & Yoshitake, M. (2007). Adsorption properties of water vapor on sulfonated perfluoropolymer membranes. *International Journal of Hydrogen Energy*, 32(3) 371-379.

Vetter, R., & Schumacher, J. (2019). Free open reference implementation of a two-phase pem fuel cell model. *Computer Physics Communications*, 234:223–234.

Wagner, W., & Pruß, A. (2002). The IAPWS Formulation 1995 for the Thermodynamic Properties of Ordinary Water Substance for General and Scientific Use. *Journal of Physical and Reference Chemical Data*, 31(2) 387.

Weber, A., & Newman, J. (2004). Transport in polymer-electrolyte membranes ii. Mathematical model. *Journal of The Electrochemical Society*, 151(2):A311–A325, .